Draft version July 29, 2014
Preprint typeset using LaTeX style emulateapj v. 11/12/01

SECONDARY STAR FORMATION IN A POPULATION III OBJECT

Hajime Susa[1]

Department of Physics, Rikkyo University, Nishi-Ikebukuro, Toshimaku, Japan

Masayuki Umemura[2]

Center for Computational Sciences, University of Tsukuba, Japan

[1] susa@rikkyo.ac.jp
[2] umemura@rccp.tsukuba.ac.jp

Draft version July 29, 2014

ABSTRACT

We explore the possibility of subsequent star formation after a first star forms in a Pop III object, by focusing on the radiation hydrodynamic (RHD) feedback brought by ionizing photons as well as H_2 dissociating photons. For the purpose, we perform three-dimensional RHD simulations, where the radiative transfer of ionizing photons and H_2 dissociating photons from a first star is self-consistently coupled with hydrodynamics based on a smoothed particle hydrodynamics method. As a result, it is shown that density peaks above a threshold density can keep collapsing owing to the shielding of H_2 dissociating radiation by an H_2 shell formed ahead of a D-type ionization front. But, below the threshold density, an M-type ionization front accompanied by a shock propagates, and density peaks are radiation hydrodynamically evaporated by the shock. The threshold density is dependent on the distance from a source star, which is $\approx 10^2 \mathrm{cm}^{-3}$ for the source distance of 30pc. Taking into consideration that the extent of a Pop III object is $\approx$ 100pc and density peaks within it have the density of $10^{2-4}\mathrm{cm}^{-3}$, it is concluded that the secondary star formation is allowed in the broad regions in a Pop III object.

Subject headings: theory:early universe — galaxies: formation — radiative transfer — molecular processes — hydrodynamics

1. INTRODUCTION

In the last decade, the formation of Population III (hereafter Pop III) stars has been explored extensively (Bromm, Coppi & Larson 1999, 2002; Nakamura & Umemura 1999, 2001; Abel, Bryan, Norman 2000, 2002; Yoshida 2006). The Pop III stars can significantly affect the reionization history in the universe (Cen 2003; Ciardi Ferrara, & White 2003; Wyithe & Loeb 2004; Somerville & Livio 2003; Sokasian et al. 2004; Murakami et al. 2005), and the metal enrichment of intergalactic medium (Nakamura & Umemura 2001; Scannapieco, Ferrara, & Madau 2002; Ricotti & Ostriker 2004). In previous analyses (Tegmark et al. 1997; Fuller & Couchman 2000; Yoshida et al. 2003), it is shown that Pop III objects have the halo mass of $\approx 10^6 M_\odot$ and the extent of $\approx$ 100pc. In Pop III objects, density peaks collapse owing to H_2 cooling, forming cloud cores with the density of $10^{2-4}\mathrm{cm}^{-3}$ (Bromm, Coppi & Larson 2002). A highest peak in the halo collapses earlier to form a first Pop III star. Hence, subsequently collapsing cores are affected by the radiative feedback by the first star. However, the range of the feedback and the possibility of secondary star formation in a Pop III object are still under debate.

If a first star is distant by more than 1pc, dense cores are readily self-shielded from the ultraviolet (UV) radiation (Tajiri & Umemura 1998; Kitayama et al. 2001; Susa & Umemura 2004a,b; Kitayama et al. 2004; Dijkstra et al. 2004; Alvarez et al. 2006). Thus, the photoevaporation by UV heating is unlikely to work devastatingly. However, the photodissociating radiation (11.18-13.6eV) of hydrogen molecules (H_2) in Lyman-Werner band (LW band) can preclude the core from collapsing, since H_2 are the dominant coolant to enable the core collapse (Haiman et al. 1997; Omukai & Nishi 1999; Haiman et al. 2000; Glover & Brand 2001; Machacek et al. 2001). Hence, this may lead to momentous negative feedback.

On the other hand, ionizing radiation for hydrogen ($\geq$13.6eV) drives an ionization front (I-front), which propagates in a collapsing core. The enhanced fraction of electrons promotes H_2 formation (Shapiro & Kang 1987; Kang & Shapiro 1992; Susa et al. 1998; Oh & Haiman 2002). In particular, the mild ionization ahead of the I-front can generate an H_2 shell, which potentially shields H_2 dissociating photons (Ricotti, Gnedin, & Shull 2001). This mechanism is likely to work positively to form Pop III stars. In practice, the propagation of I-front is complex. When UV irradiates a dense core, the I-front changes from R-type on the surface to D-type inside the core. The transition occurs via an intermediate type (M-type), which is accompanied with the generation of shock (Kahn 1954). The shock can affect significantly the collapse of the core. This is a totally radiation hydrodynamic (RHD) process, which has not been hitherto explored in detail as feedback by first stars.

In this Letter, we scrutinize the radiation hydrodynamic (RHD) feedback by a first star through the propagation of I-front in a dense core. For the purpose, we solve the three-dimensional RHD, where the radiative transfer of ionizing photons as well as H_2 dissociating photons is self-consistently coupled with hydrodynamics. In §2, the key

physical processes associated with I-front propagation are overviewed. The setup of simulation is described in §3, and numerical results are presented in §4. §5 is devoted to the conclusions.

2. BASIC PHYSICS

If a collapsing core is irradiated by an ionizing source located at the distance D, the propagation speed of I-front in the core is given by

$$v_{\rm IF} = 21 \text{ km s}^{-1} \left(\frac{\dot{N}_{\rm ion}}{10^{50}{\rm s}^{-1}}\right) \left(\frac{D}{20{\rm pc}}\right)^{-2} \left(\frac{n_{\rm core}}{10^3{\rm cm}^{-3}}\right)^{-1}, \quad (1)$$

where $\dot{N}_{\rm ion}$ is the number of ionizing photons per unit time and $n_{\rm core}$ is the number density in the cloud core. The sound speed in the regions cooling by H_2 is $a_1 \approx 1$km s^{-1}, while that in the ionized regions is $a_2 \approx 10$km s^{-1}. Hence, $v_{\rm IF} > 2a_2$ for low density cores or a nearby ionizing source, and therefore I-front becomes R-type. Supposing the cloud core size $r_{\rm core}$ is on the order of $a_1\sqrt{\pi/G\rho_{\rm core}}$, the propagation time of R-type front across the core satisfies

$$t_{\rm IF} \equiv \frac{r_{\rm core}}{v_{\rm IF}} < \frac{a_1}{2a_2}\sqrt{\frac{\pi}{G\rho_{\rm core}}} < \sqrt{\frac{\pi}{G\rho_{\rm core}}}. \quad (2)$$

This means that an R-type front sweeps the core before the core collapses in a free-fall time. Thus, the core is likely to undergo photoevaporation. On the other hand, if the density of cloud core is high enough and the source distance is large, then $v_{\rm IF} < a_1^2/2a_2$ and a D-type I-front emerges. The propagation time of D-type front across the core is

$$t_{\rm IF} > \frac{2a_2}{a_1}\sqrt{\frac{\pi}{G\rho_{\rm core}}} > \sqrt{\frac{\pi}{G\rho_{\rm core}}}. \quad (3)$$

Thus, the core can collapse before the I-front sweeps the core.

The above arguments are based on the assumption that the ionizing photon flux does not change during the propagation of I-front. However, the core could be self-shielded from the ionizing radiation if $\dot{N}(\pi r_{\rm core}^2/4\pi D^2) < 4\pi r_{\rm core}^3 n_{\rm core}^2 \alpha_{\rm B}/3$, where $\alpha_{\rm B}$ is the recombination coefficient to all excited levels of hydrogen. The critical density for self-shielding is given by

$$n_{\rm shield} \simeq \left(\frac{3\dot{N}_{\rm ion}}{16\pi D^2 a_1 \alpha_{\rm B}}\sqrt{\frac{Gm_{\rm p}}{\pi}}\right)^{2/3}$$
$$= 5.1 \text{ cm}^{-3} \left(\frac{\dot{N}_{\rm ion}}{10^{50}{\rm s}^{-1}}\right)^{2/3} \left(\frac{D}{20{\rm pc}}\right)^{-4/3} \left(\frac{a_1}{1{\rm km\ s}^{-1}}\right)^{-2/3} \quad (4)$$

If $n_{\rm core} > n_{\rm shield}$, the ionizing photon flux diminishes significantly during the I-front propagation. Hence, even if the I-front is R-type on the surface of cloud core, the front can change to M-type accompanied with shock, and eventually to D-type inside the core (Kahn 1954).

In comparison to ionizing photons, H_2 dissociating (LW band) radiation is less shielded (Draine & Bertoldi 1996). The self-shielding of LW band flux ($F_{\rm LW}$) is expressed by

$$F_{\rm LW} = F_{\rm LW,0} f_{\rm sh}\left(N_{\rm H_2,14}\right) \quad (5)$$

where $F_{\rm LW,0}$ is the incident flux, $N_{\rm H_2,14} = N_{\rm H_2}/10^{14}{\rm cm}^{-2}$, and

$$f_{\rm sh}(x) = \begin{cases} 1, & x \le 1 \\ x^{-3/4}, & x > 1 \end{cases} \quad (6)$$

However, dissociating radiation could be shielded effectively if an H_2 shell forms ahead of I-front. This process is tightly coupled with the propagation of I-front.

3. SETUP OF SIMULATION

We perform radiation hydrodynamic simulations using a novel radiation transfer solver based on smoothed particle hydrodynamics (SPH) (Susa 2006). We suppose a primordial gas cloud collapsing in a run-away fashion. The chemical compositions are initially assumed to be the cosmological residual value (Galli & Palla 1998). The mass of cloud is $M_{\rm b} = 8.3 \times 10^4 M_\odot$ in baryonic mass. When the central density of cloud exceeds a certain value, $n_{\rm on}$, we ignite a $120M_\odot$ Pop III star ($\dot{N}_{\rm ion} = 1.3 \times 10^{50}{\rm s}^{-1}$), which is located at $D = 20$pc for fiducial models. We also explore the dependence on the distance of a first star by changing the relative location between a source star and a collapsing cloud. The luminosity and the effective temperature of the source star are taken from Baraffe, Heger & Woosely (2001). The fiducial models are

Model A — $n_{\rm on} = 3 \times 10^3{\rm cm}^{-3}$ with H_2 dissociating photons but without ionizing photons

Model B — $n_{\rm on} = 3 \times 10^3{\rm cm}^{-3}$ with ionizing and H_2 dissociating photons

Model C — same as Model B but for $n_{\rm on} = 3 \times 10^2{\rm cm}^{-3}$

The physical simulation time after the ignition of the source star is 4Myr except 1.54Myr for model B, since the central part collapses below the resolution limit. In Model A, it is assumed that only LW band photons escape from the neighbor of a source star, whereas ionizing photons do not because of large opacity. This model also can be regarded as the reference to Model B.

4. RESULTS

4.1. *Failed Collapse (Model A)*

In Fig. 1, the time evolution of density profiles along the axis of symmetry is shown for three models. In this figure, the red curve represents the distribution at 1Myr, at which epoch the spatial distributions of physical quantities are shown in Fig. 2. For Model A, as shown in the left panel of Fig. 1, the collapse of central regions stops virtually and forms a quasi-hydrostatic core between ∼1Myr and ∼4Myr. The failure of collapse is caused by the photodissociation of H_2 by LW band photons. In upper panels of Fig. 2, the spatial distribution of H_2 fraction on a slice along the symmetry axis is shown by colored dots at the positions of SPH particles. In lower panels of Fig. 2, physical quantities along the symmetry axis are shown at this epoch. In Model A (left panel), the temperature is several 10^2K in the envelope and $\sim 10^3$K in the central regions. The H_2 column density is lower than $10^{14}{\rm cm}^{-2}$ in the envelope and therefore H_2 is highly photodissociated by LW band radiation. In the central regions, H_2 column density exceeds $10^{14}{\rm cm}^{-2}$ and therefore H_2 fraction is raised up by the self-shielding of LW band photons according to (5). However, this level of shielding is not enough to allow the cloud to keep collapsing by H_2 cooling. Eventually, the collapse is halted by the thermal pressure. The numerical results of Model A show that gravitational instability is hindered by permeated H_2 dissociating photons.

4.2. *H_2 Shielded Collapse (Model B)*

In Model B, ionizing photons are included for the same model parameter as Model A. In this model, I-front propagates into the cloud. Although the I-front is R-type far from the cloud center, it changes to M-type and a shock is generated as shown by a peak at 0.5Myr in Fig. 1 (middle panel). Around 1Myr, the I-front changes to D-type, and therefore the core collapse proceeds faster than the propagation of the I-front, as argued in §2. The density distribution is highly changed by photoionization, as shown by the angelfish-shaped distribution in Fig. 2. In particular, it is worth noting that an H_2 shell forms ahead of the I-front due to the enhanced ionization fraction. As a result, the H_2 column density is steeply raised up. This H_2 shell effectively shields LW band radiation from a source star, and the resultant H_2 fraction (y_{H_2}) becomes larger by an order of magnitude than that of Model A. Eventually, due to H_2 cooling, the cloud core can continue to collapse to the level of $n_H > 10^7 cm^{-3}$, as shown in Fig. 1 (middle). Since the only difference between Models A and B is the presence of ionizing radiation, we can conclude that photoionization can restrain the negative feedback effect by H_2 photodissociation.

4.3. *Shock-driven Evaporation (Model C)*

Model C is the lower density version of Model B, where n_{on} is ten times smaller than that of Model B. In this case, quite similarly to Model B, the I-front becomes to M-type at 0.5Myr (Fig. 1, right panel). As shown in Fig. 2, there forms an H_2 shell that shields LW band radiation from a source star. But, before the core collapses in the free-fall time, the shock accompanied with M-type I-front sweeps up the central regions at $\approx$ 1Myr. Eventually, the shock blows out the collapsing core. Hence, it is concluded that if an M-type I-front passes through the cloud core, the whole cloud is evaporated radiation hydrodynamically by the shock.

4.4. *Dependence on Position of a Source Star*

As shown above, the criterion of radiation hydrodynamic evaporation of a collapsing core is whether an M-type I-front sweeps up the core. By changing the position of a source star, we can obtain the threshold density for the evaporation depending on the source distance. As a result of numerical simulations, it is shown that the threshold density is $\approx 10^3 cm^{-3}$ for $D = 20$pc, $\approx 10^2 cm^{-3}$ for $D = 30$pc, and $\approx 10 cm^{-3}$ for $D = 50$pc. Thus, cloud cores with $n_{core} \gtrsim 10^2 cm^{-3}$ can collapse at $D \gtrsim 30$pc. Further details of the analysis on the parameter dependence will be described in the forth-coming full paper.

5. CONCLUSIONS

We have performed three-dimensional radiation hydrodynamic simulations to scrutinize the feedback by a first star in a Pop III object. As a result, it has been found that a collapsing core is evaporated by a shock if an M-type I-front sweeps the core. In order for a collapsing core to evade the radiation hydrodynamic evaporation, the core density should exceed a threshold density that depends on the distance from a source star. Above the threshold density, the I-front is quickly changed to the D-type, and an H_2 shell forms ahead of the I-front, which effectively shields H_2 dissociating radiation from a source star. Eventually, the core can keep collapsing owing to H_2 cooling. The present numerical study has shown that if a source star is distant by more than 30pc, then a collapsing core denser than $\approx 10^2 cm^{-3}$ is absolved from evaporation. Taking into account that the density of cloud cores in a Pop III object is expected to be $10^{2-4} cm^{-3}$, stars can form in the regions of $\gtrsim 30$ pc even after a first star forms. Since the extent of a Pop III object is $\approx$ 100pc, it is concluded that the subsequent star formation is allowed in the broad regions in a Pop III object.

We are grateful to N. Shibazaki for continuous encouragement, to T. Nakamoto and K. Ohsuga for intense discussion, and to all the collaborators in *Cosmological Radiative Transfer Codes Comparison Project* (astro-ph/0603199) for fruitful discussions during the workshop in CITA and Lorentz Center in Leiden. The analysis has been made with the *FIRST* simulator at Center for Computational Sciences in University of Tsukuba and with computational facilities in Rikkyo University. This work was supported in part by Grants-in-Aid, Specially Promoted Research 16002003 and Young Scientists (B) 17740110 from MEXT in Japan.

REFERENCES

Abel, T., Bryan, G. L., & Norman, M. L. 2000, ApJ, 540, 39
Abel, T., Bryan, G. L., & Norman, M. L. 2002, Science, 295, 93
Alvarez, M. A., Bromm, V., & Shapiro, P. R. 2006, ApJ, 639, 621
Baraffe, I., Heger, A. & Woosely, S.E. 2001, ApJ, 550, 890
Bromm, V., Coppi, P. S., & Larson, R. B. 1999, ApJ, 527, L5
Bromm, V., Coppi, P. S., & Larson, R. B. 2002, ApJ, 564, 23
Cen, R. 2003, ApJ, 591, L5
Ciardi, B., Ferrara, A., & White, S. D. M. 2003, MNRAS, 344, L7
Dijkstra, M., Haiman, Z., Rees, M. J., & Weinberg, D. H. 2004, ApJ, 601, 666
Draine, B. T., & Bertoldi, F. 1996, ApJ, 468, 269
Fuller, T. M., & Couchman, H. M. P. 2000, ApJ, 544, 6
Galli D. & Palla F. 1998, A&A, 335, 403
Glover, S. C. O., & Brand, P. W. J. L. 2001, MNRAS, 321, 385
Haiman, Z., Rees, M. J., & Loeb, A. 1997, ApJ, 476, 458
Haiman, Z., Abel, T., & Rees, M. J. 2000, ApJ, 534, 11
Kahn, F. D. 1954, Bull. Astron. Inst. Netherlands, 12, 187
Kang, H., & Shapiro, P., ApJ, 386, 432
Kitayama, T., Susa, H., Umemura, M., & Ikeuchi, S. 2001, MNRAS, 326, 1353
Kitayama,T., Yoshida, N., Susa, H. & Umemura, M., 2004, ApJ, 613, 631
Machacek, M. E., Bryan, G. L., & Abel, T. 2001, ApJ, 548, 509
Murakami, T., Yonetoku, D., Umemura, M., Matsubayashi, T., & Yamazaki, R. 2005, ApJ, 625, L13
Nakamura F. & Umemura M. 1999, ApJ, 515, 239
Nakamura, F., & Umemura, M. 2001, ApJ, 548, 19
Oh, P & Haiman, Z. 2002, ApJ, 569, 558
Omukai, K. & Nishi, R. 1999, ApJ, 518, 64
Ricotti, M. Gnedin, N. Y., Shull, M. 2001, ApJ, 560, 580
Ricotti, M. & Ostriker, J. P. 2004, MNRAS, 350, 539
Scannapieco, E., Ferrara, A., & Madau, P. 2002, ApJ, 574, 590
Shapiro, P.R., & Kang, H., 1987, ApJ, 318, 32
Sokasian, A., Yoshida, N., Abel, T., Hernquist, L., & Springel, V. 2004, MNRAS, 350, 47
Somerville, R. S. & Livio, M. 2003, ApJ, 593, 611
Susa, H. 2006, PASJ, in press (astro-ph/0601642)
Susa, H., Uehara, H., Nishi, R., & Yamada, M. 1998, Prog. Theor. Phys., 100, 63
Susa, H. & Umemura, M. 2004a, ApJ, 600, 1
Susa, H. & Umemura, M. 2004b, ApJ, 610, 5L

Tajiri, Y., & Umemura, M. 1998, ApJ, 502, 59
Tegmark, M., Silk, J., Rees, M. J., Blanchard, A., Abel, T., & Palla, F. 1997, ApJ, 474, 1
Wyithe, J. S. B., & Loeb, A. 2004, Nature, 427, 815
Yoshida, N., Abel, T., Hernquist, L. & Sugiyama, N., 2003, ApJ, 592, 645
Yoshida, N. 2006, New Astronomy Review, 50, 19

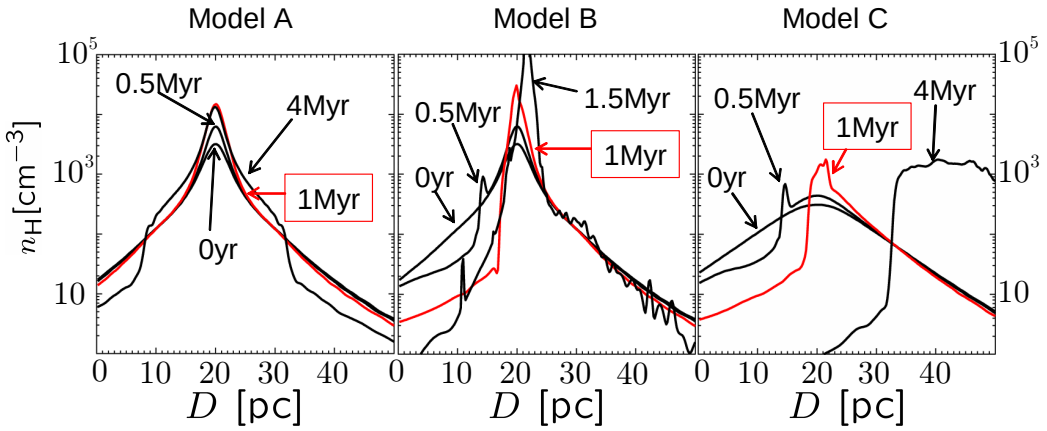

FIG. 1.— The time evolution of density distributions along the symmetry axis for three models. Four curves correspond to $t = 0$, 0.5Myr, 1Myr, and 4Myr, for models A and C, whereas the final plot for model B corresponds to $t = 1.5$Myr. The red curves denote the profiles at 1Myr, at which epoch the detailed structure is shown in Fig.2.

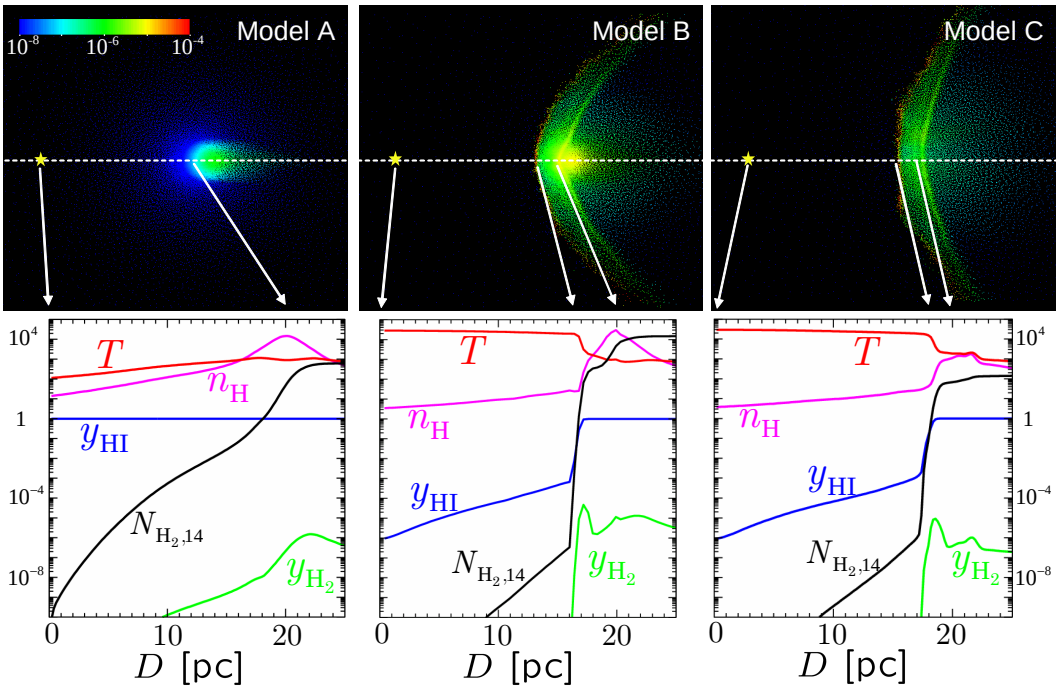

FIG. 2.— Spatial distributions of physical quantities for three models at 1 Myr. Colored dots on upper three panels represent the distributions of SPH particles on a slice which includes the symmetry axis (dashed line). The colors of particles denote the H_2 fraction, whose legend is shown on the upper left. The yellow star represents the position of a source Pop III star. Lower three panels show various physical quantities along the symmetry axis as T[K], $n_{\rm H}$[cm^{-3}], $y_{\rm HI}$, $y_{\rm H_2}$, and $N_{\rm H_2,14}$(H_2 column density from the source star in units of 10^{14}cm^{-2}). Horizontal axis shows the distance from the source star. Arrows show the correspondence of coordinates between the SPH distributions and the horizontal axis.